The Cryosphere Discussions

Snow accumulation variability in Adelie Land (East Antarctica) derived from radar and firn core data. A 600 km transect from Dome C

D. Verfaillie, M. Fily, E. Le Meur, O. Magand, B. Jourdain, L. Arnaud, and V. Favier

Laboratoire de Glaciologie et Géophysique de l'Environnement, UMR5183, Saint-Martin-d'Hères, France

Correspondence to: D. Verfaillie (dverfaillie@lgge.obs.ujf-grenoble.fr)

Title Page

Abstract | Introduction

Conclusions | References

Tables | Figures

◄◄ | ►►

◄ | ►

Back | Close

Full Screen / Esc

Printer-friendly Version

Interactive Discussion

Abstract

Polar ice sheets mass balance is a timely topic intensively studied in the context of global change and sea-level rise. However, obtaining mass balance estimates in Antarctica in particular, remains difficult due to various logistical problems. In the frame-
5   work of the TASTE-IDEA program, labeled as an International Polar Year project, continuous Ground Penetrating Radar (GPR) measurements were carried out during a traverse realised in Adelie Land (East Antarctica) during the 2008–2009 austral summer between the Italo-French Dome C (DC) polar plateau site and French Dumont D'Urville (DdU) coastal station. The aim of this study was to process and interpret GPR data
10 in terms of snow accumulation, to analyse its spatial and temporal variability along the DC-DdU traverse and compare it with historical data and modeling. The emphasis has been put on the last 300 yr, from the pre-industrial to recent time period. Beta-radioactivity counting and gamma spectrometry were studied in cores at LGGE laboratory, providing a depth-age calibration for radar measurements. Over the 600 km
15 of usable GPR data, depth and snow accumulation were determined with the help of three distinct layers visible on the radargrams (≈1730, 1799 and 1941 AD). Preliminary results reveal a gradual accumulation increase towards the coast and the occurrence of previously undocumented undulating structures between 300 and 600 km from DC. Results agree fairly well with data from previous studies and modeling. Concluding
20 on temporal variations is difficult because of the margin of error introduced by density estimation. This study should have various applications such as for model validation.

1   Introduction

Polar regions play a significant role in the climate system. Large ice sheets located over Greenland and Antarctica influence water cycle and thermohaline circulation through
25 the capture or release of freshwater. They also are crucial for Earth radiation budget due to high snow and ice albedos. Hence, in the context of global climate change

Snow accumulation variability in Adelie Land (East Antarctica)

D. Verfaillie et al.

(Solomon et al., 2007), particular attention is being paid to the mass balance of Polar ice sheets.

In order to predict ice-sheets behaviour under future climate conditions (i.e. their contribution to future sea-level rise), it is necessary (1) to assess their past and current state and (2) to understand the physical processes linking climate to the ice sheet mass balance. For this task, ice cores give precious information on quaternary climate and atmospheric composition. However, getting the accurate Antarctic mass balance remains a difficult task. This is mainly achieved through field mass balance measurements or modeling. Mass balance is the algebraic sum of two terms: the accumulation of snow on the surface of the ice sheet (through precipitation, hoar formation and wind deposition), which can be complemented by some refreezing at its base, and its ablation (through sublimation, surface and basal melting, wind scouring and iceberg calving). Surface mass balance (SMB) only refers to processes occurring at the surface of the ice sheet.

However, SMB in Antarctica remains poorly known. For instance, a slight increase in surface elevation has been observed in the interior of the continent, suggesting a recent mass gain (e.g., Helsen et al., 2008), whereas Antarctic precipitation has not undergone any significant change since the 1950s (Monaghan et al., 2006a). This contradiction points out the uncertainty of SMB measurements and interpretations, which results in a high level of incertitude concerning its future contribution to sea level rise (Meehl et al., 2007).

Various ground-based techniques are used to determine SMB in Antarctica, such as stake farms or lines, ultrasonic sensors, snow pits and firn/ice cores (Eisen et al., 2008). Density is an important parameter which has to be known accurately, as well as the depth vs. age relationship. The latter can be determined by layer counting, radiochronology (decay of natural radioactive isotopes such as ^{210}Pb) or the determination of reference horizons (volcanic layers or radioactive horizons resulting from the atmospheric nuclear weapon tests carried out between the 1950s and the 1980s) (Eisen et al., 2008; Magand, 2009).

D. Verfaillie et al.

However, all of these methods yield rather localised data and thus suffer from a poor spatial representativeness. Ground Penetrating Radar (GPR), on the other hand, offers the possibility to determine SMB continuously over several hundreds of kilometers. It is thus a powerful tool to assess its spatial (and temporal) variability and can be used to
5 make the link between firn/ice cores or stakes SMB measurements.

The aim of our study is thus to contribute to a better knowledge of East-Antarctic SMB by analysing new data (radar and firn cores) obtained along a transect between the Italo-French Concordia Dome C polar station (DC) and the French Dumont-Durville station (DdU) (Fig. 1). This round-trip traverse was made from 20 January to 10 Febru-
10 ary 2009 as part of the ANR-VANISH (Vulnerability of the ANtarctic Ice-SHeet) and IPEV-TASTE-IDEA (Trans-Antarctic Scientific Traverses Expeditions – Ice Divide of East Antarctica) scientific programs. During this traverse, (nearly) continuous radar measurements were carried out and 6 firn cores (16.5 to 21 m) were drilled (Fig. 1). Beta-radioactivity counting and gamma spectrometry from these cores made at LGGE
15 laboratory (Laboratoire de Glaciologie et Géophysique de l'Environnement) provide a depth-age calibration for radar measurements.

This transect is among the most documented ones in East Antarctica. Indeed, this traverse route has been followed regularly and studied since the 1970s (see for example the works of Pourchet et al., 1983, and Pettré et al., 1986). However, data in this
20 region are not evenly distributed. SMB measurements have been carried out regularly in the coastal area since 2004 (Genthon et al., 2007; Agosta et al., 2011; Favier et al., 2011). Other studies, on the other hand, have focused on the DC sector (Petit et al., 1982; Urbini et al., 2008). Frezzotti et al. (2004, 2005) used snow radar as well as other methods (stake farms, ice cores, surface morphology and remote sensing) to estimate
25 the SMB spatial and temporal variability along a transect from Terra Nova Bay to DC, and from D66 to Talos Dome (Magand et al., 2004). However, SMB measurements between DC and the coast are sparse and no SMB radar measurements had ever been obtained along the DC-DdU traverse.

The objective of the current study was to process and interpret the radar data in terms of SMB, to analyse its spatial and temporal variability along the DC-DdU traverse and compare it with historical data in the region. We focused on the pre-industrial to industrial time period, which spans the last 300 yr (thus approximately the first 70 m of snow, or the first 750 ns of the radargrams).

Section 2 deals with the available radar and firn core data and the various methods used in this study. The results are subsequently displayed and discussed in Sect. 3.

2 Data and methods

2.1 Radar

Ground-Penetrating Radar (GPR), also referred to as ice-penetrating radar, snow radar or radio echo sounding is a technique widely employed in various fields such as engineering, archeology, seismic exploration, glaciology... It is used for mapping the internal structures of a substrate, or locating objects in the case of archeology and construction engineering (Daniels, 2000; Eisen et al., 2008). The key advantage of this method is that it provides a continuous measurement, in contrast with other widely used glaciological SMB measurements such as stakes or firn/ice cores.

A transmitter and receiver antenna, separated by a constant distance (common offset), are trailed behind the vehicle along the survey transect. It is usually combined with GPS measurements to obtain geographical position. At fixed time intervals (in our case every second), the transmitting antenna emits an electromagnetic pulse, which penetrates into the snow. When the electromagnetic wave reaches a layer with a different complex dielectric constant ϵ^*, it is partly reflected. This reflected signal is then received by the second antenna at the surface, and the two-way travel time (TWT) of the signal (from the surface to the interface and from the interface back to the surface) is recorded (Eisen et al., 2008). Although it is still unclear how continuous reflecting

horizons are produced by the GPR in firn and ice, they have been proven isochronous by different authors and methods (Eisen et al., 2008 and references therein).

During the traverse, a 100 MHz-frequency emitting antenna was used, with a common offset of 2 m.

The GPR produces radargrams, which are a representation of all the traces recorded along a section, with the horizontal axis representing the horizontal position and the vertical axis the two-way travel time (TWT) of the wave. Radargrams were processed with a specially dedicated software called ReflexW©. Time cut, time zero correction and signal processing (gain and filters) were carried out.

Sadly, the quality of the radar measurements declined from 7 February to 9 February 2009, probably due to a deterioration of the antenna. On 10 February, the antenna was replaced and the resulting radargrams are visible again. But the reflectors cannot be followed across this blind passage, making the radargrams from 7 February to the end of the transect unusable. So we decided to analyse the profiles by starting from DC and carried on as far as possible (i.e. until 6 February a.m.). A summary of the radar data is displayed in Table 1 and the analysed radar section in Fig. 1.

Several steps are necessary to obtain accumulation values from a radargram:

1. Process the radargram in order to enhance visibility of the reflecting horizons and apply two corrections (time zero and geometrical corrections).

2. Convert the radargram vertical scale from time (TWT) to depth (see Sect. 2.4.2).

3. Pick several visible reflectors along the profile, as close as possible to dated layers of interest (i.e. volcanic or radioactive layers, see Sect. 2.3).

4. Date these reflectors from firn core interpretation.

5. Transform the snow thickness between two isochrones (or between one and the surface) into water equivalent depth and divide the latter by the time interval between the two isochrones (or the isochrone and the surface), as explained in Sect. 2.4.3.

A yearly averaged snow accumulation value is thus obtained.

The minimum radar vertical resolution is usually evaluated as $\lambda/4$ (Eisen et al., 2008), which means that we were able to set apart two reflectors if they were separated by a distance of at least 75 cm.

2.2 Firn cores

Six firn cores were drilled along the transect, in order to calibrate radar measurements with a depth-age relationship at specific points. This depth vs. age relationship is obtained by means of beta radioactivity counting to detect the radioactive layers of 1955 ± 1 and 1965 ± 1 corresponding to the fallout of the atmospheric nuclear weapon tests carried out in the 1950's and 1960's (Magand, 2009). Additional deeper core data (D47 and DC) were also used for density analysis (described in Sect. 2.4.2). A summary of the main core characteristics and radioactive layers depth is available in Table 2.

2.3 Picking reflectors

Three visible reflectors were selected for each profile in ReflexW (labeled R1 to R3). Each one was manually picked and followed along the first profile (starting from DC) and from one profile to the next. It was possible to merge two consecutive radargrams to ensure the continuity of a reflector from one profile to the next. Depths were then calculated from the TWT as will be explained in Sect. 2.4.2. Picked reflectors are displayed in Fig. 2.

Tracking of the reflectors was possible until the end of radargram 17, approximately 600 km from DC (as explained before). However, tracking of reflectors R2 and R3 turned out to be difficult at the end of radargram 12 (~465 km from DC), due to a very bad visibility of the radargram occurring there, and additional signal processing was applied to this radargram (dilatation and deconvolution filters) to enhance visibility. Hence, by using a deeper reflector visible before and after the blind gap as a marker, we were

able to find back these two reflectors at the end of the profile. Nevertheless, R2 and R3 depth (and as a result accumulation) values after 470 km from DC remain uncertain.

2.4 Density

2.4.1 Density estimates

Density is a crucial element in this study, as it will influence both the wave propagation speed in the snow and thus the conversion from TWT to depth (Sect. 2.4.2) and the final accumulation result (Sect. 2.4.3). If on the one hand the influence of density on depth estimates is moderate, on the other hand its impact on accumulation will be more drastic. Depths of our reflectors go down to 70 m. As a result, we need to estimate density beyond maximum depths of cores F2 to F4 (10 to 20 m). To estimate density as a function of depth and distance from DC, we thus chose to make use of two deep cores drilled at DC and D47 (Table 2). DC and D47 density measurements were fitted (third order polynomial fit) and density at each point along the transect was interpolated as a function of distance between those two sites.

Figure 3 provides an illustration of computed and measured density at DC, D47 and F2 to F4. Our fit method does not allow us to reproduce exactly the density values measured close to the surface, due to extreme density variability in the first layers of snow. However, fitted values remain close to measured values in the first meters of snow (inside the measurements error bars), and reproduce well measured values beyond a depth of 4 to 5 m.

2.4.2 From density to wave speed and resulting conversion from TWT to depth

In order to convert TWT into depth, the knowledge of the radar wave speed is necessary. The latter is mainly controlled by snow density.

The electromagnetic wave propagation in a media is described as:

$$c = c_v / \sqrt{\epsilon^*} \tag{1}$$

where c is wave speed in the media, c_v is wave speed in the vacuum ($= 0.3\,\mathrm{m\,ns^{-1}}$) and e^* is complex media dielectric constant. The latter is defined by:

$$e^* = e' - \mathrm{i}e'' \tag{2}$$

where e' is the real part, called complex permittivity and mainly influenced by density, and e'' is the imaginary part, mainly controlled by conductivity (Eisen et al., 2008). The imaginary part of the dielectric constant is mainly affected by the presence of liquid water (Urbini et al., 2001) and the snow chemistry. Hence, this term can be neglected for our study because the Antarctic plateau is considered to be dry and "clean". Thus, in this case:

$$e^* = e' \tag{3}$$

and, by combining Eqs. (1) and (3), we obtain:

$$c = c_v / \sqrt{e'} \tag{4}$$

Kovacs et al. (1995) proposed the following empirical approximation based on comparison of permittivity and density measurements:

$$e' = (1 + 0.845 \times \rho)^2 \tag{5}$$

Finally, by introducing Eq. (5) into Eq. (4), we obtain the following expression:

$$c = \frac{c_v}{1 + 0.845 \times \rho} \tag{6}$$

This last expression is then used to determine wave speed vs. depth at the cores on basis of density. Wave speed is then used to transform TWT into depth. A geometrical correction is necessary in the upper part of the profile so as to take into account the fact that the emitter and receiver antennas are separated by a common-offset of 2 m.

Various error sources can affect depth estimates, mainly wave speed estimates (density uncertainties, firn depth correction), time-zero correction and picking of the reflectors. Considering these error sources, we estimate a depth uncertainty of about 1 m.

2.4.3 From density to accumulation

Density values are used to transform accumulation in centimeters of snow into accumulation in cm water equivalent (we) as follows:

$$a = \int_{z_{n-1}}^{z_n} \frac{s \times \rho(z)}{z_n - z_{n-1}} dz \qquad (7)$$

where n is the number of the considered reflector R, z is depth, s is accumulation in cm of snow, a is accumulation in cm we, and ρ is density.

2.5 Dating reflectors

Dating of the picked reflectors by direct interpolation between two layers of known age at DC was not possible. Indeed, the snow surface in the surroundings of the station as well as on the traverse route is constantly modified by the passage of vehicles and manutention work and then the "real" surface does not correspond to what would be the "natural" undisturbed 2009 surface. Depths measured with the radar thus refer to the disturbed real surface and not to the natural one, impeding simple dating of reflectors. Only in the vicinity of firn core sites is the surface intact and, as the radar vehicle had to leave the traverse route to get close to those sites, the surface displayed on radargrams is natural on a short distance. This is clearly visible on the radargram close to the F4 firn core (Fig. 4). Therefore, in order to date the reflectors, we had to use in a complementary way the F4 site where the surface is natural and the DC core where some layers are well-dated.

At DC, as explained above, absolute depths of picked reflectors are not correct but the depth intervals between reflectors (R1-R2 and R2-R3) make sense. Besides, well-dated volcanic layers (Table 3) in the 2004 EPICA Dome C ice core provide a depth-age scale at DC. Depths were determined for 2004, the year the EPICA ice core was drilled.

Then data from GLACIOCLIM-SAMBA observatory stakes measurements[1] at DC were used to account for the 43 cm of snow accumulated between 2004 and 2009. Knowing the depth-age relationship at DC (Fig. 5) the age interval between the reflectors can be calculated. As the curve is non-linear the uncertainty on the absolute depths induces an uncertainty on the age interval but this error remains pretty small: an error of 1 m on the location of the reflectors induces a 3 % difference on the age intervals. We then have a time interval of 142 ± 4 yr between R1 and R2, and 69 ± 2 yr between R2 and R3.

At F4 a 10 m core was drilled, 1955 and 1965 radioactive horizons were determined, the density profile was measured and then the 2009–1955 snow accumulation is computed (Table 4). The R1, R2 and R3 depths are obtained from radargrams and then the R1-R2 and R2-R3 snow accumulation rate in $cm\,a^{-1}$ (Table 4) is calculated.

The 1955-R1 snow accumulation rate at F4 is not known a priori, it is interpolated between the 1955–2009 ($15.0\,cm\,snow\,a^{-1}$) and the R1-R2 ($11.7\,cm\,snow\,a^{-1}$) ones which make sense because the values are relatively close. From this snow accumulation rate we obtain the R1-1955 time interval and, finally, the R1, R2, R3 layers age, respectively 1941 ± 1, 1799 ± 5 and 1730 ± 7 AD.

3 Results

3.1 Undulating structures

The East Antarctic plateau is usually considered flat until its break in slope, located, in the study's area, ~230 km from the coast (i.e. 870 km from DC), and accumulation is assumed almost uniform until then (Pettré et al., 1986). However, it appears from GPS data (Fig. 6) that a first slope change is clear around 300 km from DC. Radargrams then show some undulating structures lying between 300 and 600 km from DC (Fig. 7).

---

[1]Website: http://www-lgge.ujf-grenoble.fr/ServiceObs/SiteWebAntarc/dc.html

Located in the middle of the plateau, 10 km wavelength undulations appear with vertical amplitudes ranging from 5 to 20 m (Fig. 7). More surprising, they seem to get amplified with depth. These structures are also visible in Fig. 6, which illustrates the evolution of surface elevation and the reflectors depth with increasing distance from DC.

3.2 Snow accumulation

Snow accumulation was studied between DC and 600 km from DC, and plotted against core data and accumulation from previous studies (Fig. 8) and models (Fig. 9). Only our 1730–1799 and 1799–1941 values are displayed, as well as core values for the period 1965–2009. 1941–2009 radar values were left out because the surface is not "natural" anymore on the traverse route (Sect. 2.5), inducing a greater margin of error for reflectors close to the surface. For example, on the traverse route close to core F4, a surface-induced accumulation error of $\sim +11\%$ was estimated for the period 1941–2009, while this error was reduced to less than +5 % and +3 % for 1799–1941 and 1730–1799 periods, respectively. We thus decided not to consider the 1941–2009 accumulation values.

It should be noted that the accumulation ratio (in cm of snow, not shown) between 1965–2009 core estimates and 1730–1799 or 1799–1941 radar estimates remains almost the same from DC to around 450 km from DC, but is greater at F2. For example, calculating the ratio $(a_1 - a_3)/a_1$ between 1965–2009 (a_1) and 1730–1799 (a_3) time periods yields values of 0.22 to 0.27 for DC to F3, while F2 value is 0.36. This could indicate an error in picking the reflectors after 470 km from DC, as explained in Sect. 2.3. Accumulation estimates beyond this point should thus be considered with caution.

Accumulation data were compared to four SMB climatologies (Fig. 9):

- We first compared our results to Arthern et al. (2006) and van de Berg et al. (2006) SMB climatologies which are currently assumed to be ones of the most defensible estimates of broad-scale pattern of SMB across Antarctica. Arthern et al. (2006) is obtained by continuous-part universal kriging of SMB field measurements over

the 1950–1990 period (Vaughan and Russell, 1997) with a background model based on passive microwaves data, whereas van de Berg et al. (2006) SMB values are results of the Regional Atmospheric Climate Model v.2 (RACMO2) which were calibrated with SMB field observations from Vaughan and Russell (1997) database. In the latter modeling, RACMO2 was run at 55 km resolution without snowdrift with lateral boundary conditions from ERA-40 (Uppala et al., 2005) for the period 1980 to 2004.

– We also compared our SMB data to ERA-Interim values. ERA-Interim is the most recent reanalysis (Simmons et al., 2006) from the European Centre for Medium-range Weather Forecasts (ECMWF), and covers the period 1989 to present. A reanalysis is the result of complex data assimilation to produce an optimal combination of observations and meteorological model results. The main advances of ERA-Interim over ERA-40 are a finer spectral truncation, improved model physics and a more efficient data assimilation system.

– Finally we compared our results to the SMB from an atmospheric global circulation model, LMDZ4 (Hourdin et al., 2006), which is the atmospheric component of the IPSL-CM4 climate system model (Marti et al., 2006) that participated in the World Climate Research Programme's Coupled Model Inter-comparison Project phase 3 (CMIP3) exercise to build the IPCC 4th assessment report (Meehl et al., 2007). The model used in the present study includes several improvements for the simulation of polar climates as suggested by Krinner et al. (1997).

4 Discussion

4.1 Undulating structures

Undulating structures visible in Figs. 6 and 7 are probably caused by a redistribution of snow by the wind, due to gravity waves that are triggered at breaks in slope (Gallée

and Pettré, 1998). This phenomenom was described in Adelie Land coastal areas by Pettré et al. (1986), where 40 km wavelength isochronal undulations were observed below the break point at 230 km from the coast. However, Pettré et al. (1986) did not find undulations further inland, and suggested that accumulation on the plateau was rather uniform. However, it has to be noted that their observations result from a 10 km spaced stakes network until 430 km from the coast (670 km from DC), and 3 core measurements between DC and 670 km from DC. Thus they were not able to capture structures with wavelengths around 10 km such as the ones we see on the radargrams. As noted earlier, another break in slope is also visible around 300 km from DC (Fig. 6). It is interesting to note that, as for Pettré's study, the undulations start just after that break in slope.

The undulations' link with local topography is clearly visible in Fig. 6. Low accumulation intervals between 450 and 470 km from DC are located in the lee of local elevation peaks (labelled A and B in Fig. 6), reflecting local strong ablation conditions due to high snow erosion rates caused by divergence in the katabatic wind field (e.g. van den Broeke et al., 2006; Favier et al., 2011). The crest of deep ondulations is located downwards (downwind) from the surface crest. This confirms that undulation crest is moving upwind as already observed by Frezzotti et al. (2002).

4.2 Spatial accumulation variations

A gradual increase in accumulation from DC to the end of the transect is observed (Figs. 8 and 9). This is consistent with previous observations in the region (see e.g. Pourchet et al., 1983; Pettré et al., 1986) and with a gradual humidity increase from DC to the coast (Bromwich et al., 2004). Moreover, great accumulation variations are featured by undulating structures described previously.

Radar and core accumulation correctly fits with most historical measurements (Fig. 8), although the various studied time periods differ. Several observations can be made:

Full Screen / Esc

Printer-friendly Version

Interactive Discussion

- Our radar accumulation results agree fairly well with measurements made within 25 km of DC by Frezzotti et al. (2004) and Urbini et al. (2008) for the period 1965–"recent", and with Urbini et al. (2008) estimates for the period 1739–2008. Differences remain within less than $1\,\mathrm{cm\,we\,a^{-1}}$, thus less than 25 %. Changes in accumulation for the last 20 yr observed by Urbini et al. (2008) cannot be verified here as radar data only allow estimations for older periods.

- Accumulation estimates made for the 1955–1972 period by Mulvaney and Wolff (1994) and Pourchet et al. (2003) are systematically higher than our radar and core estimates. On the contrary, Mulvaney and Wolff (1994) and Pettré et al. (1986) estimates for the periods 1959–1969 and 1955–1980, respectively are in good agreement with our results. In addition, Agosta et al. (2011) found little change in coastal SMB since the 1970's. This could lead to the conclusion that 1955–1972 was an anormally wet period compared to the last centuries, although this should be considered cautiously because of the uncertainties linked to the 1955–1972 historical data and our estimates. Further analysis of this specific period would be required.

Regarding model validation, all four SMB climatologies are close to our accumulation results (Fig. 9). However, differences between models can be noted:

- Arthern modeled accumulation is systematically higher than our results, indicating a wetter modeled climate. This is probably due to the fact that Arthern's accumulation map is based on available accumulation measurements. Between 200 and 500 km from DC, those correspond to Mulvaney and Wolff (1994) and Pourchet et al. (2003) data, which display higher accumulation values than our own (Fig. 8). Moreover, Pourchet's measurement around 470 km from DC could have been made on one of the undulations described earlier.

- ERA-INTERIM reanalysis, on the contrary, yield much drier results than our own. This situation is contrasting with the coastal area of Adelie Land where Agosta

et al. (2011) observed a good agreement with ERA-Interim, whereas ERA-40 yielded slightly too humid values due to larger sublimation in ERA-Interim. Nevertheless, our conclusions confirm that ERA-Interim generally yield too dry values over plateaus as observed by Agosta et al. (2012). This is also the reason why ERA-40 SMB integrated on the whole of Antarctica represents the lower limit of SMB values in the litterature (e.g. Monaghan et al., 2006b).

– van de Berg model results are in good agreement with our accumulation estimates. Their climatology is refitted by altitude intervals on Vaughan and Russell (1997) data, thus it does not correspond to kriging. As a result, unlike Arthern et al. (2006), their method does not introduce local biases due to old measurements made in our study region. This points to the role of biases introduced by doubtful measurements in SMB extra- and interpolations, and confirms the necessity of a data quality control, such as proposed by Magand et al. (2007).

– Qua model, LMDZ4 is "free from any meteorological observational constraint" (Agosta et al., 2011). However, it is the model which agrees the best with our accumulation values, remaining within the margin of uncertainty of our 1965–2009 core estimates. It reacts particularliy well in the study region, as observed previously in the coastal area (Agosta et al., 2011), which is surprising because "models that use observed sea-ice, such as ERA, are expected to do better in depicting the absolute amount of precipitation than climatic models, since precipitation and evaporation rates are dependent on the sea-ice extent" (Agosta et al., 2011).

4.3 Temporal accumulation variations

Temporal variations must be interpreted with caution. Indeed, density is used to convert accumulation in cm into cm we (as explained in Sect. 2.4.3). Accumulation in cm of snow (not shown) and in cm we (Figs. 8 and 9) show very different evolution with time, due to snow densification. Considering the uncertainty margin on our accumulation results (which can be considered at least equal to the core estimates' uncertainties,

11 to 17 %), accumulation in cm we shows no significant increase with time. Indeed, if (1) dating of layers at DC based on the EPICA Dome C ice core and (2) our density estimates are considered valid, no accumulation variation can clearly be noted between the three studied periods (radar 1730–1799, radar 1799–1941 and firn cores 1965–2009). However, because of the density estimation challenge, concluding on the temporal variability of accumulation is difficult.

5 Conclusions and outlook

A radar transect was carried out in Adelie Land (East Antarctica) in 2008–2009, between DC station and the coast and six complementary firn cores were drilled. This long and continuous radar dataset is one of the few obtained in the region.

Study of the 600 km-long usable dataset yields two major preliminary results.

The first result is the fact that accumulation increases gradually when moving away from DC, which is consistent with findings from previous studies in this region. Regarding spatial accumulation variations, historical accumulation data and results from modeling studies along the transect are in good agreement with our results.

The second result is the occurrence of previously undocumented 10 km wavelength undulations in a region lying between 300 and 600 km from DC. These should be analysed further in future studies, notably via atmospherical modelling (MAR model, Gallée and Schayes, 1994), assuming the model can capture such a fine resolution. It also provides an indication for the search of new drilling sites. We now know that the section from 450 to 500 km from DC would not be suitable for drilling a new core because of its high accumulation variability.

The third and last result relates to temporal accumulation variations. No significant accumulation change with time can be noted, if dating of layers at DC based on the EPICA Dome C ice core and our density estimates are considered valid. Indeed, accumulation results rely heavily on density estimates, and as a result, concluding on the temporal evolution of accumulation is difficult. Density measurements are punctual and

Snow accumulation variability in Adelie Land (East Antarctica)

D. Verfaillie et al.

Title Page

Abstract | Introduction

Conclusions | References

Tables | Figures

◀ | ▶|

◀ | ▶

Back | Close

Full Screen / Esc

Printer-friendly Version

Interactive Discussion

often not deep enough. We took advantage of two deep cores drilled at DC and D47 (1000 km appart) to estimate density along the transect, as an interpolation in function of the distance to those two sites.

In the long term, a density measurement method rapid to carry out should be developped to ensure more frequent density measurements. This would be useful not only for this study, but for every study which needs precise density estimates.

New radar and firn core measurements were obtained during a transect between DC and Vostok stations in 2011–2012. Upcoming analysis of these new data should offer complementary knowledge about East-Antarctic SMB.

INSU
Institut national des **sciences** de **l'Univers**

References

Agosta, C., Favier, V., Genthon, C., Gallée, H., Krinner, G., Lenaerts, J., and van den Broeke, M.: A 40-year accumulation dataset for Adelie Land, Antarctica and its application for model validation, Clim. Dynam., 38, 75–86, doi:10.1007/s00382-011-1103-4, 2011. 2858, 2869, 2870

Agosta, C., Favier, V., Genthon, C., Gallée, H., and Krinner, G.: High resolution modeling of the Antarctic surface mass balance, Part I: Model description and validation, Clim. Dynam., submitted, 2012. 2870

Arthern, R., Winebrenner, D., and Vaughan, D.: Antarctic snow accumulation mapped using polarization of 4.3-cm wavelength microwave emission, J. Geophys. Res., 111, D06107, doi:10.1029/2004JD005667, 2006. 2866, 2870

Bromwich, D., Guo, Z., Bai, L., and Chen, Q.: Modeled antarctic precipitation. Part I: Spatial and temporal variability, J. Climate, 17, 427–447, 2004. 2868

Castellano, E., Becagli, S., Hansson, M., Hutterli, M., Petit, J. R., Rampino, M. R., Severi, M., Steffensen, J. P., Traversi, R., and Udisti, R.: Holocene volcanic history as recorded in the sulfate stratigraphy of the European Project for Ice Coring in Antarctica Dome C (EDC96) ice core, J. Geophys. Res., 110, D06114, doi:10.1029/2004JD005259, 2005. 2879

Daniels, J.: Ground Penetrating Radar Fundamentals, prepared as an appendix to a report to the US EPA, Region V, Department of Geological Sciences, The Ohio State University, 2000. 2859

Eisen, O., Frezzotti, M., Genthon, C., Isaksson, E., Magand, O., Broeke, M., Dixon, D., Ekaykin, A., Holmlund, P., Kameda, T., Karlöf, L., Kaspari, S., Lipenkov, V., Oerter, H., Takahashi, S., and Vaughan, D.: Ground-based measurements of spatial and temporal variability of snow accumulation in East Antarctica, Rev. Geophys., 46, RG2001, doi:10.1029/2006RG000218, 2008. 2857, 2859, 2861, 2863

Favier, V., Agosta, C., Genthon, C., Arnaud, L., Trouvillez, A., and Gallée, H.: Modeling the mass and surface heat budgets in a coastal blue ice area of Adelie Land, Antarctica, J. Geophys. Res., 116, F03017, doi:10.1029/2010JF001939, 2011. 2858, 2868

Frezzotti, M., Gandolfi, S., and Urbini, S.: Snow megadunes in Antarctica: sedimentary structure and genesis, J. Geophys. Res., 107, 4344, doi:10.1029/2001JD000673, 2002. 2868

Frezzotti, M., Pourchet, M., Flora, O., Gandolfi, S., Gay, M., Urbini, S., Vincent, C., Becagli, S., Gragnani, R., Proposito, M., Severi, M., Traversi, R., Udisti, R., and Fily, M.: New estimations of precipitation and surface sublimation in East Antarctica from snow accumulation measurements, Clim. Dynam., 23, 803–813, 2004. 2858, 2869

Frezzotti, M., Pourchet, M., Flora, O., Gandolfi, S., Gay, M., Urbini, S., Vincent, C., Becagli, S., Gragnani, R., Proposito, M., Severi, M., Traversi, R., Udisti, R., and Fily, M.: Spatial and temporal variability of snow accumulation in East Antarctica from traverse data, J. Glaciol., 51, 113–124, 2005. 2858

Snow accumulation variability in Adelie Land (East Antarctica)

D. Verfaillie et al.

Title Page

Abstract	Introduction
Conclusions	References
Tables	Figures

|◄ | ►|

◄ | ►

Back | Close

Full Screen / Esc

Printer-friendly Version

Interactive Discussion

Gallée, H. and Pettré, P.: Dynamical constraints on katabatic wind cessation in Adélie Land, Antarctica, J. Atmos. Sci., 55, 1755–1770, 1998. 2867

Gallée, H. and Schayes, G.: Development of a 3-dimensional meso-gamma primitive equation model – katabatic winds simulation in the area of terra-nova bay, Antarctica, Mon. Weather Rev., 122, 671–685, 1994. 2871

Genthon, C., Lardeux, P., and Krinner, G.: The surface accumulation and ablation of a blue ice area near Cap Prudhomme, Adélie Land, Antarctica, J. Glaciol., 53, 635–645, 2007. 2858

Helsen, M., van den Broeke, van de Wal, R., van de Berg, W., van Meijgaard, E., Davis, C., Li, Y., and Goodwin, I.: Elevation changes in Antarctica mainly determined by accumulation variability, Science, 320, 1626–1629, 2008. 2857

Hourdin, F., Musat, I., Bony, S., Braconnot, P., Codron, F., Dufresne, J.-L., Fairhead, L., Filiberti, M.-A., Friedlingstein, P., Grandpeix, J.-Y., Krinner, G., LeVan, P., Li, Z.-X., and Lott, F.: The LMDZ4 general circulation model: climate performance and sensitivity to parametrized physics with emphasis on tropical convection, Clim. Dynam., 27, 787–813, 2006. 2867

Kovacs, A., Gow, A., and Morey, R.: The in-situ dielectric constant of polar firn revisited, Cold Reg. Sci. Technol., 23, 245–256, 1995. 2863

Krinner, G., Genthon, C., Li, Z., and Le Van, P.: Studies of the Antarctic climate with a stretched-grid general circulation model, J. Geophys. Res., 102, 13,731–13,745, 1997. 2867

Magand, O.: Bilan de masse de surface Antarctique: techniques de mesure et analyse critique, Ph.D. thesis, Université Joseph Fourier, Grenoble, 2009. 2857, 2861

Magand, O., Frezzotti, M., Pourchet, M., Stenni, B., Genoni, L., and Fily, M.: Climate variability along latitudinal and longitudinal transects in East Antarctica, Ann. Glaciol., 39, 351–358, 2004. 2858

Magand, O., Genthon, C., Fily, M., Krinner, G., Picard, G., Frezzotti, M., and Ekaykin, A.: An up-to-date quality-controlled surface mass balance data set for the 90°–180° E Antarctica sector and 1950–2005 period, J. Geophys. Res., 112, D12106, doi:10.1029/2006JD007691, 2007. 2870

Marti, O., Braconnot, P., Bellier, J., Benshila, R., Bony, S., Brockmann, P., Cadule, P., Caubel, A., Denvil, S., Dufresne, J.-L., Fairhead, L., Filiberti M.-A., Fichefet, T., Foujols, M.-A., Friedlingstein, P., Grandpeix, J.-Y., Hourdin, F., Krinner, G., Lévy, C., Madec, G., Musat, I., De Noblet, N., Polcher, J., and Talandier, C.: The new IPSL climate system model: IPSL-CM4, Note du Pôle de Modélisation IPSL, ISSN, Note du Pôle de Modélisation, 26, 1288–1619, 2006. 2867

Title Page

Abstract | Introduction

Conclusions | References

Tables | Figures

◄ | ►

◄ | ►

Back | Close

Full Screen / Esc

Printer-friendly Version

Interactive Discussion

Meehl, G., Stocker, T., Collins, W., Friedlingstein, A., Gaye, A., Gregory, J., Kitoh, A., Knutti, R., Murphy, J., Noda, A., Raper, S. C. B., Watterson, I. G., Weaver, A. J. and Zhao, Z.-C: Global climate projections, in: Climate Change 2007: The Physical Science Basis. Contribution of Working Group I to the Fourth Assessment Report of the Intergovernmental Panel on Climate Change, edited by: Solomon, S., Qin, D., Manning, M., Chen, Z., Marquis, M., Averyt, K., Tignor, M., and Miller, H., Cambridge University Press, 2007. 2857, 2867

Monaghan, A., Bromwich, D., Fogt, R., Wang, S., Mayewski, P., Dixon, D., Ekaykin, A., Frezzotti, M., Goodwin, I., Isaksson, E., Kaspari, S., Morgan, V., Oerter, H., Van Ommen, T., Van der Veen, C., and Wen, J.: Insignificant change in Antarctic snowfall since the International Geophysical Year, Science, 313, 827, doi:10.1126/science.1128243, 2006a. 2857

Monaghan, A., Bromwich, D., and Wang, S.: Recent trends in Antarctic snow accumulation from Polar MM5 simulations, Philos. T. R. Soc. A, 364, 1683–1708, 2006b. 2870

Mulvaney, R. and Wolff, E.: Spatial variability of the major chemistry of the Antarctic ice sheet, Ann. Glaciol., 20, 440–447, 1994. 2869

Petit, J., Jouzel, J., Pourchet, M., and Merlivat, L.: A detailed study of snow accumulation and stable isotope content in Dome C (Antarctica), J. Geophys. Res., 87, 4301–4308, 1982. 2858

Pettré, P., Pinglot, J., Pourchet, M., and Reynaud, L.: Accumulation distribution in Terre Adélie, Antarctica: effect of meteorological parameters, J. Glaciol., 32, 486–500, 1986. 2858, 2865, 2868, 2869

Pourchet, M., Pinglot, F., and Lorius, C.: Some meteorological applications of radioactive fallout measurements in Antarctic snows, J. Geophys. Res., 88, 6013–6020, 1983. 2858, 2868

Pourchet, M., Magand, O., Frezzotti, M., Ekaykin, A., and Winther, J.: Radionuclides deposition over Antarctica, J. Environ. Radioactiv., 68, 137–158, 2003. 2869

Simmons, A., Uppala, S., Dee, D., and Kobayashi, S.: ERA-Interim: new ECMWF reanalysis products from 1989 onwards, ECMWF Newsl., 110, 25–35, 2006. 2867

Solomon, S., Qin, D., Manning, M., Chen, Z., Marquis, M., Averyt, K., Tignor, M., and Miller, H.: IPCC, 2007: Climate Change 2007: The Physical Science Basis. Contribution of Working Group I to the Fourth Assessment Report of the Intergovernmental Panel on Climate Change, 2007. 2857

Uppala, S., Kallberg, P., Simmons, A., and collaborators: The ERA-40 re-analysis, Q. J. Roy. Meteor. Soc., 131, 2961–3012, 2005. 2867

Urbini, S., Vittuari, L., and Gandolfi, S. A.: GPR and GPS data integration: examples of application in Antarctica, Ann. Geofis., 44, 687–702, 2001. 2863

Snow accumulation variability in Adelie Land (East Antarctica)

D. Verfaillie et al.

Back | Close

Full Screen / Esc

Printer-friendly Version

Interactive Discussion

Urbini, S., Frezzotti, M., Gandolfi, S., Vincent, C., Scarchilli, C., Vittuari, L., and Fily, M.: Historical behaviour of Dome C and Talos Dome (East Antarctica) as investigated by snow accumulation and ice velocity measurements, Global Planet. Change, 60, 576–588, 2008. 2858, 2869

van de Berg, W., van den Broeke, M., Reijmer, C., and van Meijgaard, E.: Reassessment of the Antarctic surface mass balance using calibrated output of a regional atmospheric climate model, J. Geophys. Res., 111, D11104, doi:10.1029/2005JD006495, 2006. 2866, 2867

van den Broeke, M., van de Berg, W. J., van Meijgaard, E., and Reijmer, C.: Identification of Antarctic ablation areas using a regional climate model, J. Geophys. Res., 111, D18110, doi:10.1029/2006JD007127, 2006. 2868

Vaughan, D. and Russell, J.: Compilation of Surface Mass Balance Measurements in Antarctica, Internal Rep. ES4/8/1/1997/1, British Antarctic Survey, Cambridge, UK, 1997. 2867, 2870

Discussion Paper | Discussion Paper | Discussion Paper | Discussion Paper

Table 1. Summary of the radar data from DC to the coast. Gaps in the data are due to technical problems encountered during the traverse. The unusable data starting at 597 km from DC is due to a deterioration of the antenna, as explained in the text. See Fig. 1 for explanation about the profiles' numbering.

Distance from DC	Date interval	Comments
0 to 138 km	2 Feb a.m.–3 Feb a.m.	radargrams 1–6
138 to 194 km	3 Feb a.m.–3 Feb p.m.	no data
194 to 250 km	3 Feb p.m.	radargrams 7–8
250 to 270 km	3 Feb p.m.–4 Feb a.m.	no data
270 to 597 km	4 Feb a.m.–6 Feb a.m.	radargrams 9–17
597 to 1100 km	6 Feb a.m.–10 Feb p.m.	unusable data

Table 2. Firn and ice cores used in this study: name, drilling year, coordinates, altitude in m above sea level (a.s.l.), distance from DC station, total drilling depth, depth of 1955 and 1965 radioactive layers in 2009. DC data is a compilation of various datasets. 1955 and 1965 depth at DC are based on the 2004 EPICA Dome C core depths. Corresponding depths in 2009 have been estimated by using stake measurements from GLACIOCLIM-SAMBA observatory, as explained in Sect. 2.5.

Name	Year	Coordinates (lat. S)	(long. E)	Altitude (m a.s.l.)	Distance from DC (km)	Total depth (m)	1955 depth (m)	1965 depth (m)
D47	1987–1989	67° 23′ 00	138° 43′ 00	1548	999	897	–	–
F6	2008–2009	68° 44′ 70	134° 54′ 53	2430	788	21	–	18–18.5
F1	2008–2009	70° 08′ 32	134° 08′ 01	2630	650	20.4	–	18–18.5
F2	2008–2009	71° 02′ 50	133° 01′ 17	2830	551	19.38	14–14.5	12–12.5
F3	2008–2009	71° 56′ 13	131° 17′ 42	3030	433	18.35	–	7.5–8
F4	2008–2009	72° 54′ 17	129° 10′ 17	3178	304	10	7–7.2	6–6.2
F5	2008–2009	73° 58′ 27	126° 34′ 51	3204	164	10.1	6.1–6.2	5–5.2
DC	1999–2008	75° 06′ 00	123° 21′ 00	3233	0	–	5.0	4.4

Table 3. Characteristic volcanic layers in the EPICA Dome C core: name, age, depth at DC in 2004 (adapted from Castellano et al., 2005) and estimated depth at DC in 2009 (for an undisturbed surface).

Layer name	Age	Depth at DC in 2004 (m)	Estim. depth at DC in 2009 (m)
Agung	1964 ± 1	3.9	4.4
Tambora	1816 ± 4	12.5	12.9
Jorullo-Taal	1758 ± 6	15.36	15.8
Serua	1696 ± 4	18.62	19.05

Table 4. Summary of the parameters which were measured or computed at F4 to calculate ages, and ensueing computed age for each reflector.

Layers	Intervals	Measured depth (cm)	Depth interval (cm)	Snow accu (cm a^{-1})	Time interval (yr)	Computed age
	1955–2009		700–720	15.00 (measured)	54	
1955		700–720				
	R1–1955		173–193	13.33 (interpolated)	14 ± 1 (computed)	
R1		893				1941 ± 1
	R1-R2		1655	11.65 (measured)	142 ± 4 (from DC core)	
R2		2548				1799 ± 5
	R2-R3		746	10.82 (measured)	69 ± 2 (from DC core)	
R3		3294				1730 ± 7
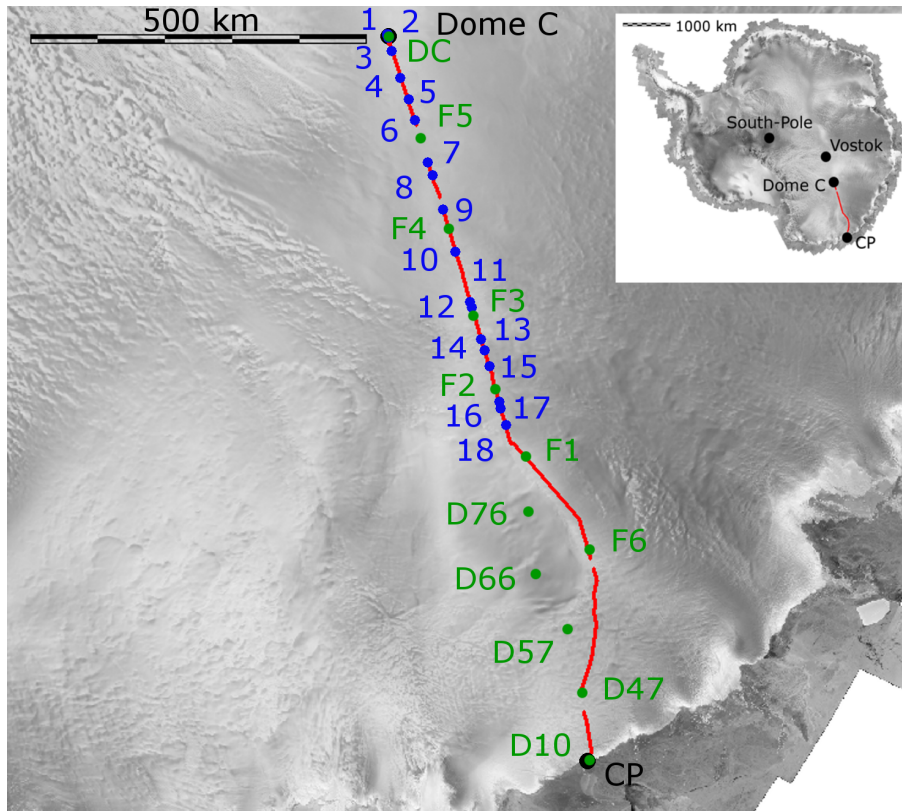
Fig. 1. Map of Antarctica displaying the location of the analysed radar section (number 1 to 18, in blue) and cores (in green). Each blue number corresponds to the beginning of a radargram. A general map of Antarctica is inserted in the top right corner to indicate the major scientific stations on the Antarctic plateau and East Antarctica, as well as the traverse made between DC and Dumont-d'Urville (Cap Prud'Homme is indicated on the map instead of Dumont-d'Urville, located on an island 5 km offshore).

Title Page

Abstract | Introduction

Conclusions | References

Tables | Figures

|◄ | ►|

◄ | ►

Back | Close

Full Screen / Esc

Printer-friendly Version

Interactive Discussion

Fig. 2. Picked reflectors labeled R1 to R3 shown on radargram 5. Distance is in meters
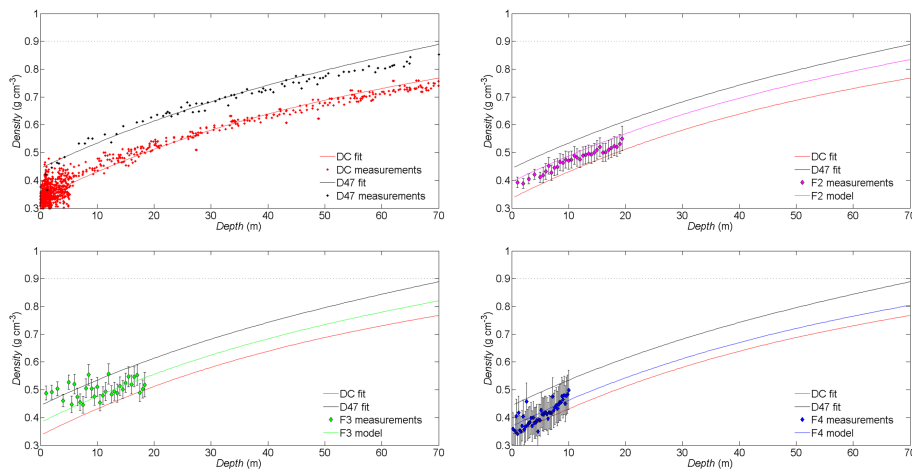
Fig. 3. Density as a function of depth. Density measurements up to 70 m-depth and their fits are represented at DC and D47 (top left panel). Measured and computed density at F2 (top right), F3 (lower left) and F4 (lower right) are also displayed. Error bars for DC and D47 measurements are not represented for clarity purposes, but have the same order of magnitude as for shallower cores F2 to F4 (∼10 % error).
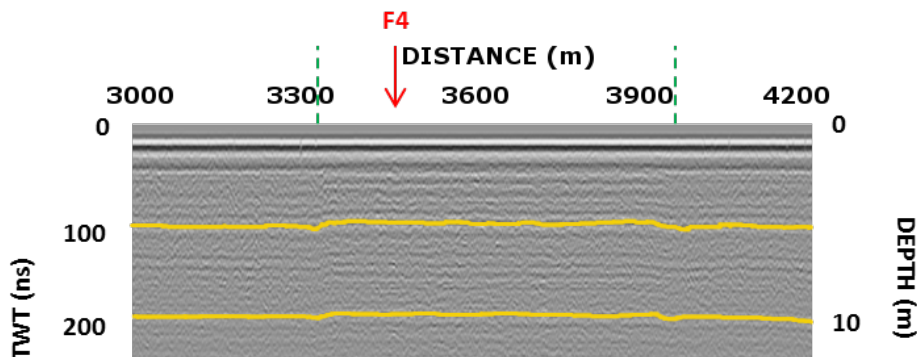
Fig. 4. Transition between "real" and "natural" snow surface visible on radargram 9 in the vicinity of core F4. The first dotted line corresponds to the point where the radar vehicle left the traverse route and the second one to the point where it got back to the traverse route.

$$y = -3E\text{-}05x^2 - 0{,}1134x + 2012{,}7$$
$$R^2 = 0{,}999$$
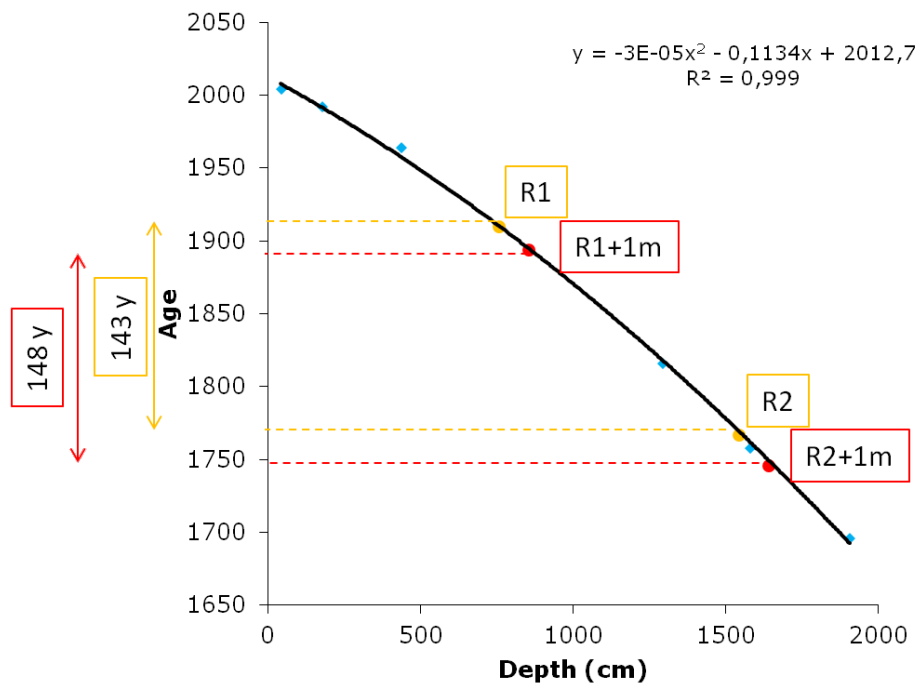
Fig. 5. 2009 Depth-age relationship at DC (black curve) based on dating of EPICA Dome C volcanic layers (blue markers). The age interval between reflectors R1 and R2 is shown, as well as the age interval between those two reflectors if a 1 m-shift in depth is applied.
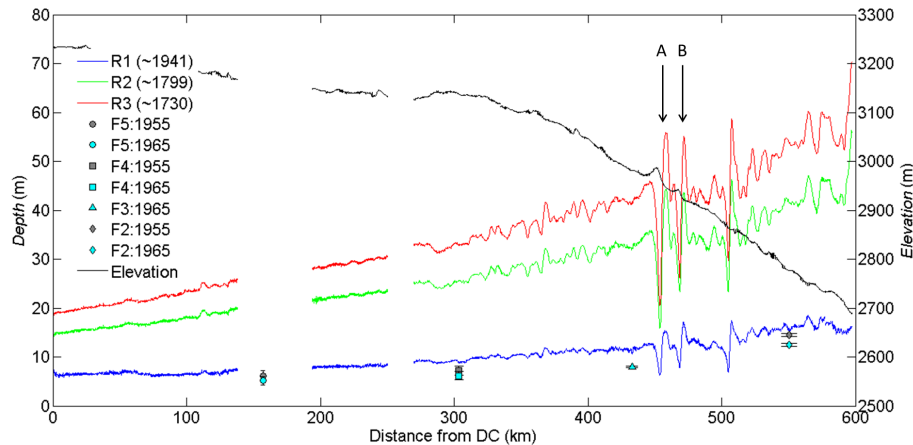
Fig. 6. Reflectors' depth and surface elevation vs. distance from DC. Markers represent depths of 1955 and 1965 layers measured on the cores for a comparison, and their associated error bars.
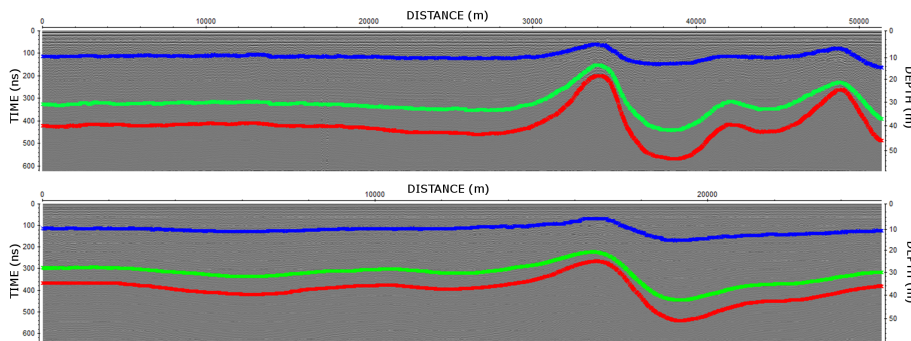
Fig. 7. Undulating structures visible on radargrams number 12 (5 February a.m., between 450 and 470 km from DC) and 14 (5 February p.m., between 495 and 510 km from DC).
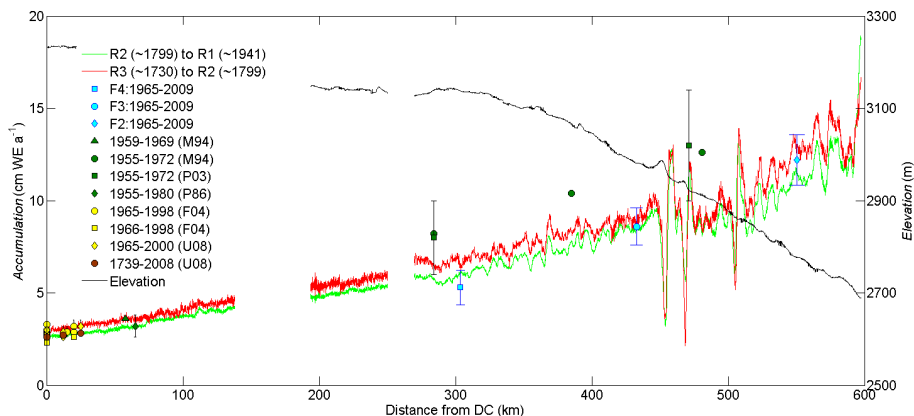
Fig. 8. Comparison between our accumulation results (radar and core measurements) and results from other studies carried out previously along the transect. M94 = Mulvaney et al., 1994; P03 = Pourchet et al., 2003; P86 = Pettré et al., 1986; F04 = Frezzotti et al., 2004; U08 = Urbini et al., 2008.
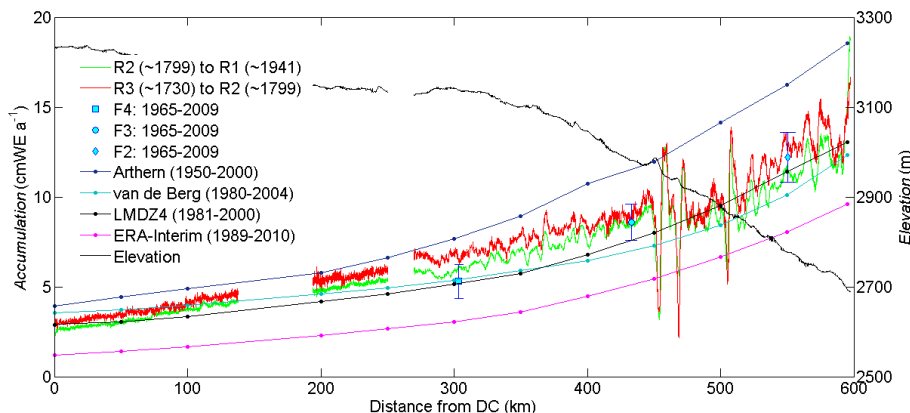
Fig. 9. Comparison between our accumulation results (radar and core measurements) and modeling results along the transect.